# Journal of Applied Sciences

ISSN 1812-5654

science alert

ANSInet
an open access publisher
http://ansinet.com

Journal of Applied Sciences 12 (5): 440-449, 2012
ISSN 1812-5654 / DOI: 10.3923/jas.2012.440.449


# An Analytical Closed Form Solution Around Underground Openings Using Different Methods

[1]O. Saeidi, [2]A. Elyasi, [1]S. Maleki and [3]A. Fegh
[1]School of Mining Engineering, Shahrood University of Technology, Shahrood, Iran
[2]Rock Mechanics College, Tarbiat Modares University, Tehran, Iran
[3]School of Mining, University of Tehran, Tehran, Iran

**Abstract:** This study presents a closed form solution around underground openings based on the four rock failure criteria. The results of the closed form solution are compared to the numerical method to establish the solution. The Tresca, Mohr-Coulomb, Mogi-Coulomb and generalized Hoek-Brown failure criteria are used to determine stress distribution and plastic zone around the circular space. The solutions are implemented in three dimensional distinct element code (3DEC) and assessed numerically. Also, the parametric study using these criteria is presented. Results show that the Tresca failure criterion does not fit in rock mass problems. Because of the employing axial stress, the Mogi-Coulomb failure criterion fitted the numerical results, appropriately. It was observed that increasing the axial stress using Mogi-Coulomb failure criterion decreases the stress distribution and the plastic zone, significantly.

**Key words:** Underground circular space, rock failure criteria, stress distribution, plastic zone, 3DEC

## INTRODUCTION

During excavation in rock mass far-filed *in situ* stresses are redistributed and cause a plastic deformation around the openings such as tunnels, shafts, wellbores etc. Analytical solution in this case involves elastoplasticity which have been used in previous texts (Carranza-Torres and Fairhurst, 1999; Chen *et al*., 1999; Hoek and Brown, 1980; Li and Michel, 2009; Detournay, 1986; Carranza-Torres, 1998). Alani (2002) and Alani and Nasser (2001) developed a new cubic macro-element and quadratic analyses for plate with a hole under bending and compared with closed form solution, respectively. Exact determination of stress field in elastoplastic solution requires appropriate rock failure criterion. The medium in elasto-plastic solution for circular space presumed homogenous, compressive and isotropic far-filed stress that subjected to internal pressure, $P_i$ that applied in plane strain condition (Carranza-Torres and Fairhurst, 2000; Muhlhaus, 1985; Hoek, 1998; Malvern, 1969). Closed form solution of GRC implementing in convergence-confinement method by elasto-plastic model are among the most broadly used for general design evaluation, especially regarding excavations and support design. Taha *et al.* (2009) applied the Mohr-Coulomb material and simulated stress distribution around a pile in cohesion less soil. It was found that dry soil condition gives more resistance than others. Stress concentration analysis around a wellbore showed that in addition to rock-mud interaction drilling string vibration could cause many problems (Ibrahim *et al*., 2004). Macro element analysis and closed form solution of stress distribution around cavities in plate bending were modeled and had excellent results with regards to conventional finite element solutions (Al-Ani, 2010).

The Mohr-Coulomb criterion (M-C) was the most common criterion that has been used in elasto-plastic solution of stress state around openings (Florence and Schwer, 1978). However, The Hoek-Brown criterion (H-B) could find wide practical application as a method of describing the stress condition in rock mass surrounded the opening. Hassani *et al.* (2008) presented a 3D finite element analysis of Siah Bishe tunnels by using ABAQUS software. It was observed maximum displacement occurs in the roof of the tunnels. Stress concentration was intensified in transition zone of tunnel and shaft. The rock mass condition under which Hoek-Brown criterion can be applied is only intact rock or heavily jointed rock masses that can be considered homogenous and isotropic (Hoek *et al*., 1998). The Classic Tresca criterion related the difference between maximum and minimum principal stresses to the cohesion without friction, like Von Mises

**Corresponding Author:** O. Saeidi, School of Mining Engineering, Shahrood University of Technology, Shahrood, Iran
Tel: +989149804239

(Hill, 1950). Stress analysis and hydro mechanical behavior of the Bisotun epigraph showed that heterogeneity is one of the most significant factors on hydraulic and mechanical properties of rock mass (Karimnia and Shahkarami, 2011). Fatigue behavior of a cylindrical hole in piston was studied by Rahman *et al.* (2009) using the Tresca and Von Mises materials. It was observed that more conservative prediction to use Signed Tresca parameter and Signed von Mises stress gives the result that lie between the absolute maximum principal stress and signed Tresca results.

Most of the cited failure criteria which applied in rock mechanics were extended before the function of the intermediate principal stress was evident. According to experimental data has shown that the intermediate principal stress has a substantial-although slight-influence on the strength of several rock classes (Colmenares and Zoback, 2002; Mogi, 1967). The Mogi-Coulomb Criterion (MG-C) clearly showed the impact of intermediate principal stress that was based on linear Mogi criterion in terms of first and second stress invariants (Al-Ajmi and Zimmerman, 2006). A mathematical model for couple coal/rock mass visco-elastic deformation was presented by Sun (2006). It could properly show the gas leak flow in these mediums.

This study concerns analytical solution of stress distribution about an underground circular space via four rock failure criteria includes the generalized Hoek-Brown, the Mohr-Coulomb, the Mogi-Coulomb and the Tresca criterion which implemented in 3DEC by means of a FISH program. The aim of this paper was to compare elasto-plastic solution of the rock failure criteria numerically in the 3DEC. Advantages and deficient of each criterion is presented. In addition, parametric study of the rock failure criteria in elasto-plastic solution has been carried out.

## FOUR ROCK FAILURE CRITERIA

**The Tresca criterion:** After a series of experiments, Tresca achieved that the material will failed when a critical amount of shear stress is reached (Tresca, 1868):

$$\tau_{max} = \frac{1}{2}(\sigma_1 - \sigma_3) = C \quad (1)$$

where, C is the cohesion and $\tau_{max}$ is the maximum shear stress of the material. Notice that the Tresca criterion can be considered as a particular type of the M-C criterion, with $\varphi = 0$.

**The generalized Hoek-Brown criterion:** The generalized H-B criterion concerns the maximum principal stress, $\sigma_1$ to the minimum principal stress, $\sigma_3$ via Eq. 2:

$$\sigma_1 = \sigma_3 + \sigma_c (m\frac{\sigma_3}{\sigma_c} + S)^a \quad (2)$$

where, $\sigma_c$ is the Uniaxial Compressive Strength (UCS) of intact rock, m, s and a are constants which depend on the rock mass properties:

$$m = m_i \exp(\frac{GSI - 100}{28 - 14D}) \quad (3)$$

$$s = \exp(\frac{GSI - 100}{9 - 3D}) \quad (4)$$

$$a = 0.5 + \frac{1}{6}[\exp(-\frac{GSI}{15}) - \exp(-\frac{20}{3})] \quad (5)$$

where, $m_i$ is the value of m for intact rock and can be obtained from laboratory tests. While, D is the disturbance factor which varies from 0.0 for undisturbed rock masses to 1.0 for very disturbed rock mass e.g., by stress release and drill-blast. The Geological Strength Index (GSI) introduced by Hoek indicates the characteristic of the rock mass (Hoek, 1994).

**The Mohr-Coulomb criterion:** A more general and frequently used criterion is the Mohr-Coulomb failure criterion. Failure will occur when in any (failure) plane the shear stress, $\tau$ reaches the failure shear stress, $\tau_{max}$ which is given by a functional relation of the form:

$$\tau_{max} = c + \sigma_n \tan\varphi \quad (6)$$

where, c is the cohesion of the rock mass, $\varphi$ is the internal friction angle of the rock mass and $\sigma_n$ is the normal stress working on the individual failure plane. The M-C criterion can be written with regard to the maximum and minimum principal stresses as follows (Benz and Schwab, 2008):

$$\sigma_1 = \frac{2c\cos\varphi}{(1 - \sin\varphi)} + \tan^2(\frac{\varphi}{2} + 45) \quad (7)$$

**The Mogi-Coulomb failure criterion:** All three rock failure criteria considered above, did not take into account the influence of intermediate principal stress and determined from triaxial tests. Mogi's experimental attempts revealed that rock strength varied with the intermediate principal stress, $\sigma_2$ which was obtained from polyaxial (True-Triaxial) tests (Mogi, 1971). He related the octahedral shear stress at failure to the sum of the minimum and maximum principal stresses

$$\tau_{oct} = f(\frac{\sigma_1 + \sigma_3}{2}) \quad (8)$$

where, f is a monotonically increasing function. The MG-C criterion can be stated as:

$$\tau_{oct} = a + b(\frac{\sigma_1 + \sigma_3}{2}) \quad (9)$$

According to Al-Ajmi and Zimmerman (2006) the linear Mogi parameters a and b can be related to the Coulomb shear strength parameters c and φ then can be extended as follows:

$$a = \frac{2\sqrt{2}}{3}c\cos\varphi \quad \text{and} \quad a = \frac{2\sqrt{2}}{3}\sin\varphi \quad (10)$$

## STRESSES AROUND CIRCULAR SPACE BY ELASTO-PLASTIC SOLUTION

**Elasto-plastic solution around circular space using the Tresca failure criterion:** The elasto-plastic analytical solution is commonly carries out for simplified models. Consequently as shown in Fig. 1 a circular space is utilized in plane strain condition which subjected to isotropic stresses, $\sigma_h$ and $\sigma_v$ at infinity and internal pressure $P_i$. Then, $R_i$ is the primary radius of the underground space; $R_e$ is the plastic zone radius; R and θ are the cylindrical coordinate of an assumed location, while $\sigma_R$ and $\sigma_\theta$ are the related radial and tangential stresses, respectively.

According to equilibrium equation (Jaeger *et al*., 2007):

$$\frac{d\sigma}{dr} + \frac{\sigma_r - \sigma_\theta}{r} = 0 \quad (11)$$

And it is assumed that $\sigma_\theta$, $\sigma_r$ will be $\sigma_1$ and $\sigma_3$, respectively. The Tresca failure criterion (Sec. 1.1) then requires:

$$\sigma_\theta - \sigma_R = \sigma_c, \sigma_c = 2C \quad (12)$$

in the plastic zone ($R_i$<R<$R_e$). Introducing Eq. 12 into Eq. 11 the stresses at boundary condition are given by:

$$\sigma_R = \sigma_c \ln\frac{R}{R_i} + P_i \quad (13)$$

$$\sigma_\theta = \sigma_c(\ln\frac{R}{R_i} + 1) + P_i \quad (14)$$

As the Tresca criterion does not comprise the intermediate principal stress the hydrostatic ground pressure $\sigma_v = \sigma_h$ is assumed to solve the problem. Therefore, the induced stresses in the elastic region can be found in Hiramatsu and Oka (1968) as follows:

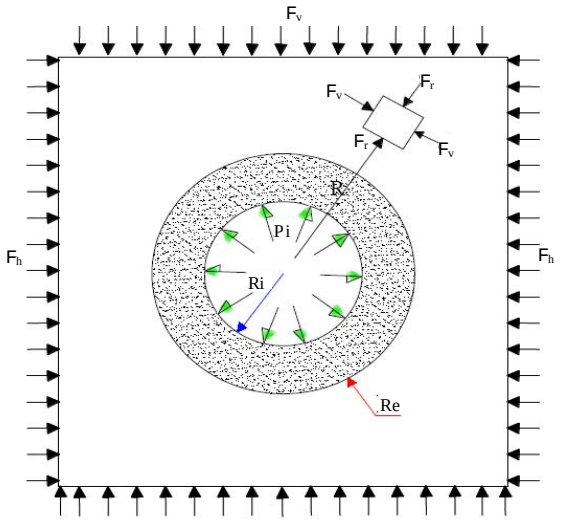


Fig. 1: The circular space subjected to isotropic stresses, $\sigma_h$ and $\sigma_v$; internal pressure, $P_i$

$$\sigma_R = \sigma_h - (\sigma_h - \sigma_{Re})(\frac{R_e}{R})^2 \quad (15)$$

$$\sigma_\theta = \sigma_h + (\sigma_h - \sigma_{Re})(\frac{R_e}{R})^2 \quad (16)$$

where, $\sigma_{Re}$ is the radial stress at elastic-plastic interface i.e. ($R = R_e$). From Eq. 15 and 16 at this interface it can be obtained:

$$\sigma_{\theta e} + \sigma_{Re} = 2\sigma_h \quad (17)$$

Substituting Eq. 17 into Eq. 12 the induced radial stress can be determined as follows:

$$\sigma_{Re} = \sigma_h - \frac{\sigma_c}{2} \quad (18)$$

The plastic zone radius is determined from Eq. 18 and 13 as:

$$R_e = R_i \exp(\frac{\sigma_h - P_i}{\sigma_c} - \frac{1}{2}) \quad (19)$$

Assumed the circular space with $R_i$ = 1 m and $\sigma_v = \sigma_h$ = 30 MPa. Figure 2 illustrates the effects of internal pressure $P_i$ on the plastic zone radius around the circular space by the Tresca criterion for three types of rocks. The plastic zone radius decreases by increasing of UCS, while internal pressure exceeds ground pressure, the results become vice versa. For an invariable UCS, increasing the internal pressure $P_i$ decreases the plastic zone radius $R_e$.

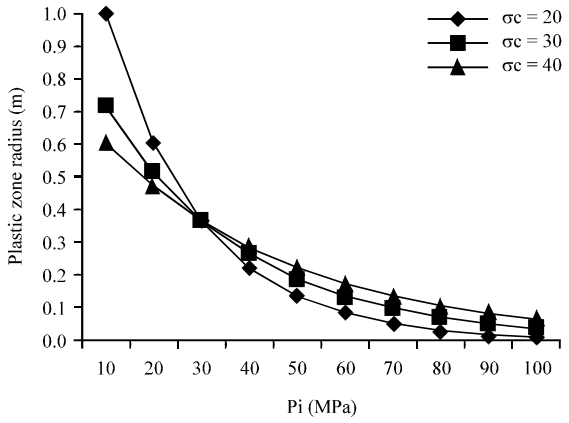


Fig. 2: The effects of internal pressure on plastic zone radius at different compressive strengths

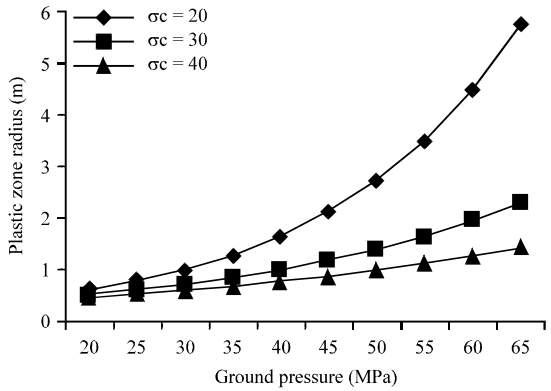


Fig. 3: The effects of hydrostatic ground pressure on the plastic zone radius at different compressive strengths

Figure 3 displays the effects of ground pressure, $\sigma_v = \sigma_h$ on the plastic zone radius by the Tresca criterion for three types of rocks where internal pressure $P_i$ is 10 MPa. An increase in ground pressure leads to increase in the plastic zone radius in an invariable UCS. It can be seen that increasing UCS tends to decrease in the plastic zone radius.

**Elasto-plastic solution around circular space using the generalized H-B failure criterion:** In the plastic region, radial and tangential stresses can be found.

Thus, induced stresses by introducing Eq. 2 into Eq. 11 are as follows:

$$\sigma_R = \frac{\sigma_c}{m}\left\{m(1-a)\ln\frac{R}{R_i} + \left[m\frac{p_i}{\sigma_c} + s\right]^{1-a}\right\}^{\frac{1}{1-a}} - s\frac{\sigma_c}{m} \quad (20)$$

$$\sigma_\theta = \sigma_R + \sigma_c\left[m\frac{\sigma_R}{\sigma_c} + s\right]^a \quad (21)$$

The radius of plastic zone can be determined from Eq. 17 and 20 that will be expressed as:

$$N1 = \exp(-(\ln(\exp(\frac{(0.7+\ln(P_0/\sigma_c))}{a}) - s)\times a^2 - 0.7 - \ln(\frac{P_0}{s_c}))/a)\times\sigma_c$$
$$N2 = (\frac{\exp(0.7+\ln(P_0/\sigma_c))}{a}) - s)^{(a-1)}\times s\sigma_c + P_i(\frac{P_i m + s\sigma_c}{\sigma_c})^{(a-1)}\times m \quad (22)$$
$$R_e = R_i(\frac{-N1+N2+((P_i m + s\sigma_c)/\sigma_c)^{(a-1)}\times s\sigma_c)}{m\sigma_c(a-1)})$$

All the parameters in this paper were assumed, where the ground pressure $P_0$ is equal to hydrostatic stresses $\sigma_v = \sigma_h$. Figure 4 shows the effects of GSI and D on the plastic zone radius by the H-B failure criterion around circular space for different rock types where, $m_i = 4$, $P_i = 10$ MPa, $\sigma v = \sigma h = 30$ MPa and $\sigma_c = 20$ MPa. An increase in the D factor for the certain GSI leads to increasing of the plastic zone radius. Whereas increasing the GSI decreases the plastic zone radius.

Figure 5 shows the effects of internal pressure on the radius of plastic zone by H-B failure criterion for different rock types where, $\sigma_v = \sigma_h = 60$ MPa, $m_i = 4$, $\sigma_c = 20$ MPa and D = 0.1. It can be understood with increasing of internal pressure the plastic zone radius will decrease in a certain GSI. Figure 6 displays the influence of the GSI on the radial stress around circular space for different rock types with $\sigma_v = \sigma_h = 50$ MPa, $m_i = 4$, $\sigma_c = 20$ MPa. It can be observed the radial stress around circular space will decrease when GSI increases.

The influence of ground pressure on tangential stress around circular space has been showed in Fig. 7 by the H-B failure criterion with $P_i = 0$, $\sigma_c = 20$ MPa, D = 05 and GSI = 20. It can be noticed that for a certain ground pressure the increasing of $m_i$ will decrease the tangential stress. On the other hand when the ground pressure increases for a fixed $m_i$ the tangential stress raises.

**Elasto-plastic solution around circular space using the Mogi-Coulomb failure criterion:** As pointed out in Sec. 1.4 the strengthening effect of the intermediate principal stress can be taking into account by utilizing the Mogi-Coulomb formula. In terms of first and second stress invariants $I_1$ and $I_2$ defined by Al-Ajmi and Zimmerman (2006):

$$I_1 = \sigma_1 + \sigma_2 + \sigma_3,\ I_2 = \sigma_1\sigma_2 + \sigma_2\sigma_3 + \sigma_1\sigma_3$$
$$(I_1^2 - 3I_2)^{1/2} = a + b(I_1 - \sigma_2) \quad (23)$$

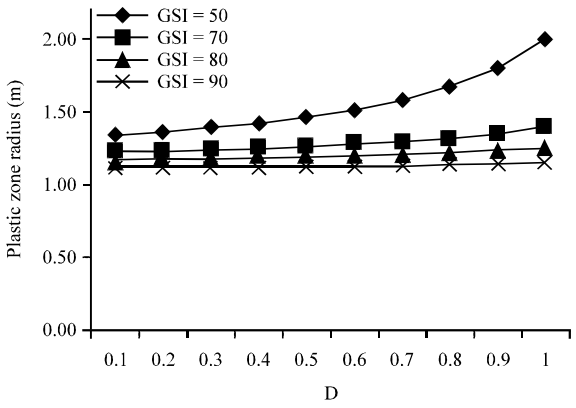


Fig. 4: Variation of the plastic zone radius with disturbance factor at different GSI using the H-B failure criterion

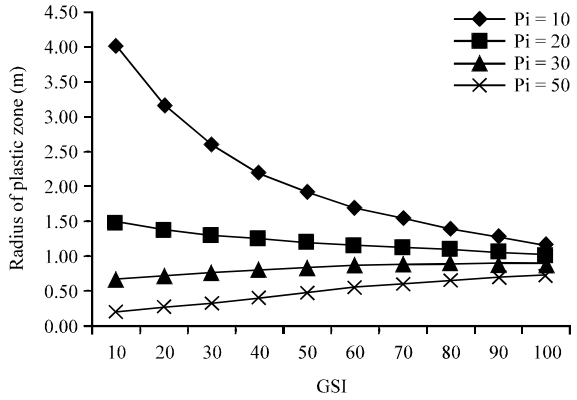


Fig. 5: Variation of the radius of plastic zone under increasing of GSI at different internal pressures by the H-B failure criterion

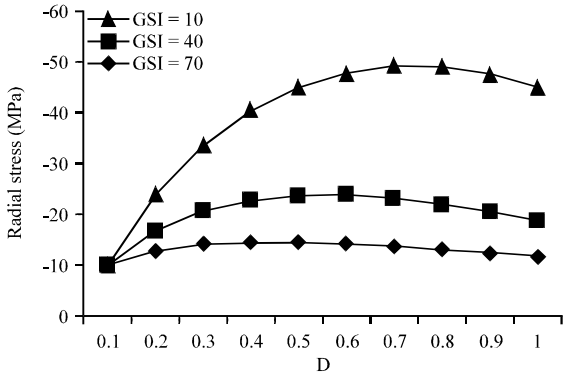


Fig. 6: The influence of D on the radial stress at different GSI around circular space using the H-B failure criterion

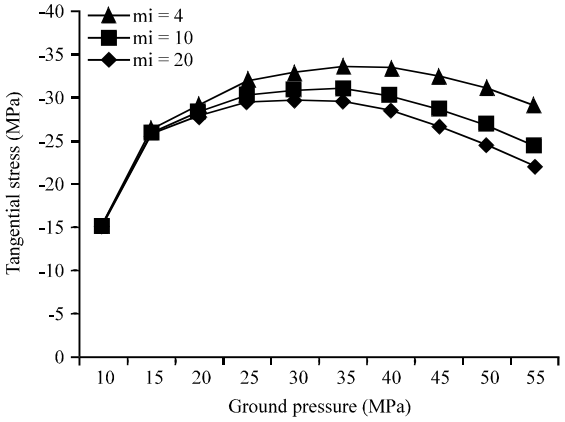


Fig. 7: The influence of ground pressure on the tangential stress at different mi around circular space using the H-B failure criterion

Since the maximum and minimum principal stresses, $\sigma_1$ and $\sigma_2$ are corresponded to $\sigma_\theta$ and $\theta_r$ around the underground circular spaces then intermediate principal stress will be $\sigma_2 = \sigma_z$ along the circular space axis. In plane strain condition ($\varepsilon_z = 0$) the axial stress, $\sigma_z$ can be determined as follows:

$$\sigma_z = \sigma_a - 2\nu\sigma_v + \upsilon(\sigma_r + \sigma_\gamma) \tag{24}$$

where, $\sigma_a$ is the axial *in situ* stress, v is the Poisson's ratio. In hydrostatic ground pressure around the circular space, $\sigma_v = \sigma_h = \sigma_a$ the Eq. 15 can be rewritten as:

$$\sigma_z = (1-2\nu)\sigma_v + \upsilon(\sigma_r + \sigma_\gamma) \tag{25}$$

The radial stress in this case can be determined through Eq. 23 and 11 as follows:

$$D1 = b^2\nu^2 + \nu - \nu^2 + b^2 + 2b^2\nu - 1$$

$$D2 = 2\ln\left(\frac{R}{R_i}\right)\left(\frac{b^2P_0\nu^2 + P_0\nu - (P_0\nu^2 - b^2\nu^2) - 0.5(b^2P_0 - ab\nu - 0.5P_0 + b^2P_0\nu)}{D1}\right)$$

$$D3 = \ln\left(\frac{R}{R_i}\right)\left(\frac{\nu^2 - b^2\nu - \nu - ba}{D1}\right)$$

$$D4 = (4b^2 - 48b^2P_0^2\nu + 48b^2P_0^2\nu^2 + 12abP_0 - 3P_0^2 + 12P_0^2\nu - 12P_0^2\nu^2 + 24P_0\nu^2)$$

$$D5 = -36abP_0\nu + 4a^2 + 12b^2P_0^2 - 4\nu a^2 + 4\nu^2a^2 + 4ab - 8ab\nu^2 + 24P_0\nu^2ba + 8b^2\nu$$

$$D6 = -24P_0\nu - 6P_0 + 12\nu - 12\nu^2 + 24b^2P_0\nu - 48b^2P_0\nu^2$$

$$s_R = (D2 + D3) \times (D4 + D5 + D6 + 20ab\nu + 16b^2\nu_2)^{0.5} - \ln\left(\frac{R}{R_i}\right) \tag{26}$$

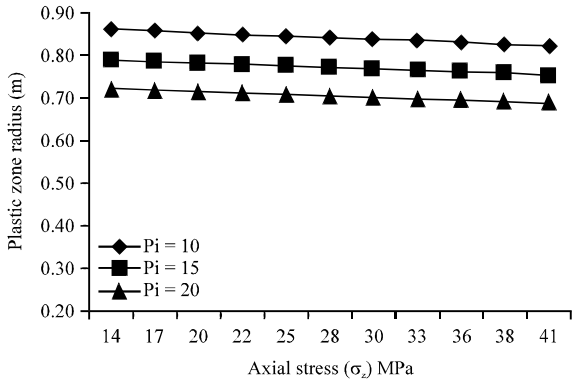


Fig. 8: The influence of axial stress on the plastic zone radius at different internal pressures around the circular space by the MG-C failure criterion

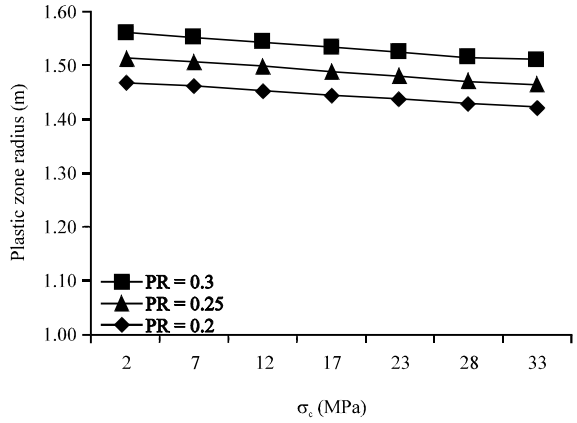


Fig. 9: The influence of compressive strength on the plastic zone radius at different Poisson's ratios around circular space using MG-C criterion

Substituting Eq. 26 and 25 into Eq. 23 the tangential stress around circular space using MG-C criterion can be found as:

$$F1 = -0.5(2ba - 2P_i + 2\sigma_R + 2b^2 - (4bas_R - 8baP_i + 8b^2\sigma_R P_i + 4b^2\sigma_R{}^2 + 4b^2P_i{}^2$$
$$\sigma_\theta = F1 + 4a^2 + 6\sigma_R b - 3\sigma_R{}^2 - 12\sigma_R P_i - 12P_i - 3a + 12ab + 12b^2)^{0.5})/(b^2 - 1) \quad (27)$$

As stated in previous sections the plastic zone radius is obtained using continues equations ($\sigma_{Re} = \sigma_R$) at elastic-plastic interface. Figure 8 represents the influence of intermediate principal stress (axial stress) on the plastic zone radius around the circular space based on the MG-C failure criterion. The features of the circular space and rock mass assumed as $R_i$ = 1 and cohesion C = 3.45 MPa, v = 0.23 and $\varphi = 30°$. It can be understood that an increase in intermediate principal stress in a certain internal pressure, causes decreasing the plastic zone radius.

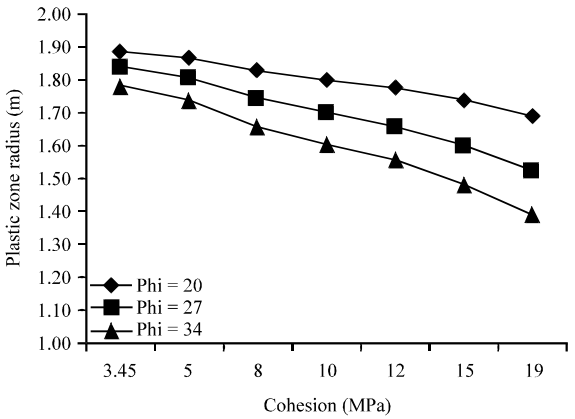


Fig. 10: Variation of the plastic zone radius under increasing rock cohesion at different friction using the MG-C criterion

Figure 9 indicates the effects of the Poisson's ratio and uniaxial compressive strength on the plastic zone radius around the circular space by using the MG-C failure criterion for different rock strengths. In this case, the internal pressure $P_i$ is 10 MPa, ground pressure $\sigma_h = \sigma_v$ is 30 MPa and the initial radius of underground space $R_i$ is 1 m. It can be obtained that the plastic zone radius increases by increasing of the Poisson's ratio in a particular UCS. Also in a fixed Poisson's ratio an increase in UCS decreases the plastic zone radius. As illustrated in Fig. 10 when cohesion of the rock around the circular space increases, in a fixed friction angle the plastic zone radius decreases. On the other hand by increasing friction angle the plastic zone radius decreases subsequently.

## NUMERICAL ANALYSIS

As a common criterion the elasto-plastic solution for the circular space using M-C failure criterion has been given in Salencon (1969). For this reason the solution has not mentioned in the previous section. Here, the analytical solution of the Tresca, generalized H-B, M-C and MG-C failure criteria implemented in 3DEC using a FISH program (ITASCA, 2003). Because of axisymmetric and plain strain conditions only one-fourth of the sketch in the Fig. 1 has been modeled.

All the parameters in these solutions were assumed, where the initial radius of the underground circular space $R_i$ is 1 m, the *in situ* stress $\sigma_h = \sigma_v$ is 30 MPa and the internal pressure $P_i$ is 5 MPa. The compressive strength of rock mass $\sigma_c$ is 50 MPa, constant parameter m is 4.5, the Geological Strength Index GSI is 40, the Poisson's ratio v is 0.22, cohesion C is 3.45 MPa and internal friction $\varphi$ is 30°. Figure 11 compares the results of the generalized H-B and Tresca failure criteria with the 3DEC.

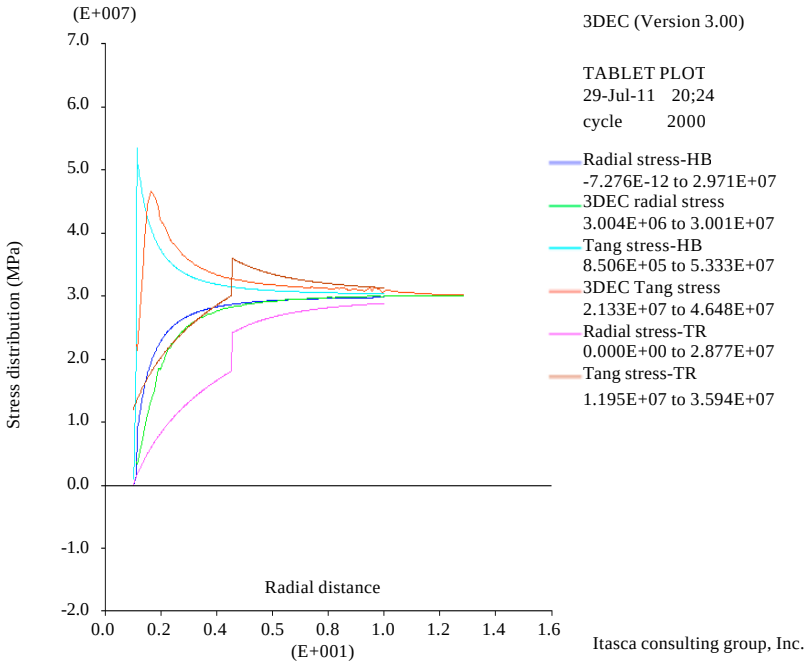


Fig. 11: The comparison of the radial and tangential stresses using the Tresca, the generalized H-B criteria with the 3DEC around the circular space

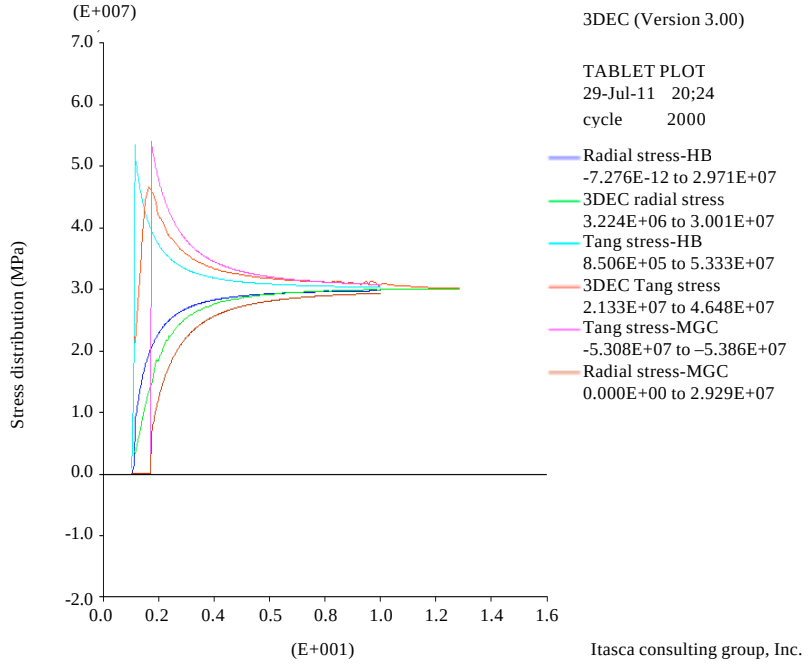


Fig. 12: The comparison of the radial and tangential stresses using the MG-C, the generalized H-B criteria with the 3DEC around the circular space

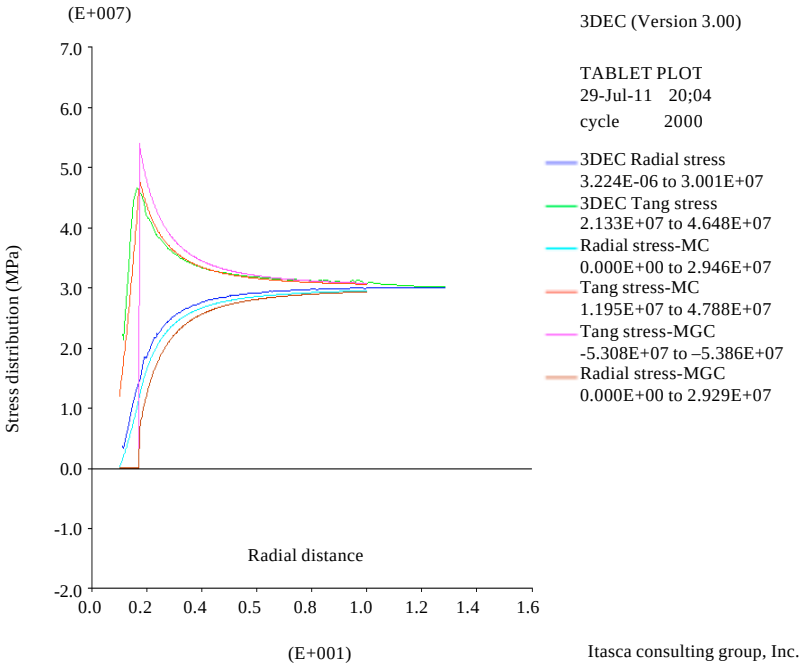


Fig. 13: The comparison of the radial and tangential stresses using the MG-C and M-C criteria with the 3DEC around the circular space

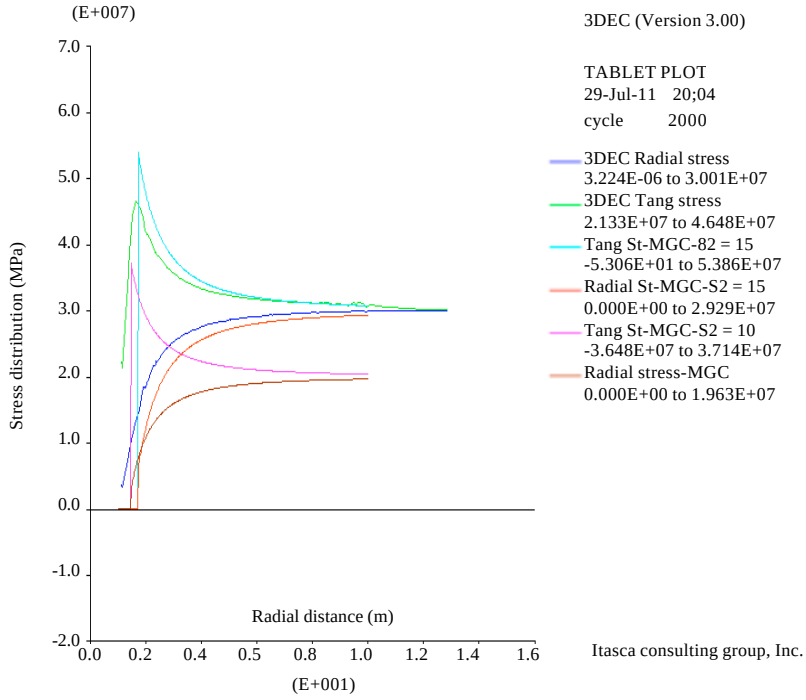


Fig. 14: The influence of intermediate principal stress using MG-C criterion ($\sigma_2 = 10$ and $\sigma_2 = 15$) on the stress distribution around the circular space

Table 1: The plastic zone radius around the circular space using four rock failure criteria compared with 3DEC

| Rock failure criteria | Tresca | Generalized Hoek-Brown | Mohr-Coulomb | Mogi-Coulomb $\sigma_2$ = 10 MPa | Mogi-Coulomb $\sigma_2$ = 15 MPa | 3DEC |
|---|---|---|---|---|---|---|
| The plastic zone radius, $R_p$ (m) | 4.5 | 1.045 | 1.73 | 1.72 | 1.45 | 1.55 |

It can be seen that stress distribution around the circular space using the generalized H-B criterion (the tangential stress in turquoise line and the radial stress in blue line) is close to the 3DEC (the tangential stress in red line and the radial stress in green line) than the Tresca criterion. Because the Tresca criterion does not concern with internal friction of the rock mass then it cannot be used in rock properties determination and the elasto-plastic solution around the underground spaces.

The results of the generalized H-B and MG-C failure criteria, compared with the 3DEC have shown in Fig. 12. The stress distribution around the circular space using the MG-C criterion (the tangential stress in turquoise line and the radial stress in brown line) is more similar to the 3DEC than the generalized H-B criterion.

In Fig. 13, the comparison of stress distribution using the MG-C and the M-C criteria has represented. The both results of criteria are similar to the 3DEC, completely. The effect of intermediate principal stress (axial stress in this case) is illustrated in Fig. 14. It can be discerned that an increase in intermediate principal stress from $\sigma_2$ = 10 MPa (the tangential stress in turquoise line and the radial stress in brown line) to $\sigma_2$ = 15 MPa (the tangential stress in cyan line and the radial stress in red line) increases the stress distribution around the circular space using the Mogi-Coulomb (MG-C) failure criterion.

The plastic zone radius around the underground circular space using four rock failure criteria are given in Table 1.

It can be found that the Tresca failure criterion overestimated the plastic zone radius more than other criteria and an increase in axial stress using MG-C failure criterion tends to decrease of the plastic zone radius. The generalized H-B failure criterion evaluated the least amount with regard to other criteria and numerical analysis in 3DEC.

## CONCLUSIONS

Elasto-plastic analytical solution of stress distribution around the underground circular space using four rock failure criteria has been given. The following consequences attained:

- The Tresca failure criterion overestimated the stress distribution and radius of the plastic zone around the underground circular space. Because of neglecting internal friction, this criterion does not answer the rock mass problems
- Increasing of uniaxial compressive strength, GSI, $m_i$ and internal pressure $P_i$ decreases the plastic zone radius and the induced stresses while an increase in ground pressure $P_0$, disturbance factor D and Poisson's ratio v increases the induced stresses and the plastic zone radius around the underground circular space
- Numerical analysis of elasto-plastic solution using four rock failure criteria has been carried out using 3DEC. The criterion that has closest fitting to 3DEC was the Mohr-Coulomb, Mogi-Coulomb and generalized Hoek-Brown failure criterion, respectively
- The advantage of Mogi-Coulomb failure criterion to the others is that comprising the axial stress (intermediate principal stress) in this criterion. It was declared that an increase in axial stress increases the stress distribution while decrease the plastic zone radius
- The generalized H-B failure criterion estimated the smallest amount of the plastic zone radius vis-à-vis other criteria and 3DEC

## REFERENCES

Al-Ajmi, A.M. and R.W. Zimmerman, 2006. Stability analysis of vertical boreholes using the Mogi-Coulomb failure criterion. Int. J. Rock Mechanics Min. Sci., 43: 1200-1211.

Al-Ani, H.R.A., 2010. Beams and plate bending macro-elements. Asian J. Applied Sci., 3: 109-134.

Alani, H.R.A. and I.B. Nasser, 2001. Development of quadratic plate bending macro-elements. Pak. J. Applied Sci., 1: 417-425.

Alani, H.R.A., 2002. Cubic macro-element for plates under bending. J. Applied Sci., 2: 1084-1091.

Benz, T. and R. Schwab, 2008. A quantitative comparison of six rock failure criteria. Int. J. Rock Mechanics Min. Sci., 45: 1176-1186.

Carranza-Torres, C. and C. Fairhurst, 1999. The elasto plastic response of underground excavations in rock masses that satisfy the Hoek Brown failure criterion. Int. J. Rock Mech. Min. Sci., 36: 777-809.

Carranza-Torres, C. and C. Fairhurst, 2000. Application of the convergence-confinement method of tunnel design to rock masses that satisfy the hoek-brown failure criterion. Tunnelling Underground Space Technol., 15: 187-213.

Carranza-Torres, C., 1998. Self-similarity analysis of the elasto-plastic response of underground openings in rock and effects of practical variables. Ph.D. Thesis, University of Minnesota.

Chen, X., C.P. Tan and C.M. Haberfield, 1999. Solutions for the deformations and stability of elastoplastic hollow cylinders subjected to boundary pressures. Int. J. Numerical Anal. Methods Geomech., 23: 779-800.

Colmenares, L.B. and M.D. Zoback, 2002. A statistical evaluation of intact rock failure criteria constrained by polyaxial test data for five different rocks. Int. J. Rock Mecha. Min. Sci., 39: 695-729.

Detournay, E., 1986. Elastoplastic model of a deep tunnel for a rock with variable dilatancy. Rock Mech. Rock Eng., 19: 99-108.

Florence, A.L. and L.E. Schwer, 1978. Axisymmetric compression of a Mohr-Coulomb medium around a circular hole. Int. J. Numerical Anal. Methods Geomech., 2: 367-379.

Hassani, H., S. Arshadnejad, H. Khodadadi and N. Goodarzi, 2008. 3D numerical modeling of a couple of power intake shafts and head race tunnels at vicinity of a rock slope in Siah Bishe pumped storage dam, North of Iran. J. Applied Sci., 8: 4294-4302.

Hill, R., 1950. The Mathematical Theory of Plasticity. Oxford University Press, Oxford.

Hiramatsu, Y. and Y. Oka, 1968. Determination of the stress in rock unaffected by boreholes or drifts, from measured strains or deformations. Int. J. Rock Mech. Min. Sci. Geomechanics Abst., 5: 337-353.

Hoek, E. and E.T Brown, 1980. Underground Excavations in Rock. MAA Publishing Company, London.

Hoek, E., P.K. Kaiser and W.F. Bawden, 1998. Underground Excavations in Hard Rock. A.A. Balkema, Rotterdam, Brookfield.

Hoek, E., 1994. Strength of rock and rock masses. ISRM News J., 2: 4-16.

Hoek, E., 1998. Reliability of Hoek-Brown estimates of rock mass properties and their impact on design. Int. J. Rock Mech. Min. Sci. Geomech. Abstr., 35: 63-68.

ITASCA, 2003. 3 Dimensional Distinct Element Code (3DEC 3.0). Itasca Consulting Group, Inc., Minnesota.

Ibrahim, A.A., T.A. Musa and A.M. Fadoul, 2004. Drilling mechanics: Consequences and relevance of drill string vibration on wellbore stability. J. Applied Sci., 4: 106-109.

Jaeger, J.C. and N.G.W. Cook and R.W. Zimmerman, 2007. Fundamentals of rock mechanics. 4th Edn., Wiley- Blackwell, Oxford.

Karimnia, M. and A. Shahkarami, 2011. Hydro mechanical coupling behavior effects on the Bisotun epigraph damaging progress. J. Applied Sci., 11: 2764-2772.

Li, L. and A. Michel, 2009. An elastoplastic evaluation of the stress state around cylindrical openings based on a closed multiaxial yield surface. Int. J. Numer. Anal. Methods Geomech., 33: 193-213.

Malvern, L.E., 1969. Introduction to the Mechanics of a Continuous Medium. Prentice-Hall, Inc., New Jersey.

Mogi, K., 1967. Effect of intermediate principal stress on rock failure. J. Geophys. Res., 72: 5117-5131.

Mogi, K., 1971. Fracture and flow of rocks under high triaxial compression. J. Geophys. Res., 76: 1255-1269.

Muhlhaus, H.B., 1985. Lower bound solutions for circular tunnels in two and three dimensions. Rock Mech. Rock Eng., 18: 37-52.

Rahman, M.M., A.K. Ariffin, M.R.M. Rejab, K. Kadirgama and M.M. Noor, 2009. Multiaxial fatigue behavior of cylinder head for a free piston linear engine. J. Applied Sci., 9: 2725-2734.

Salencon, J., 1969. Contraction quasi-statique d'une cavite a symetrie spherique ou cylindrique dans un milieu elastoplastique. Annales Des Ponts Et Chaussees, 4: 231-236.

Sun, P., 2006. A new model for coupled rock-coal deformation and gas leak flow in mining engineering. J. Applied Sci., 6: 2444-2449.

Taha, M.R., J.M. Abbas, Q.S.M. Shafiqu and Z.H. Chik, 2009. The Performance of laterally loaded single pile embedded in cohesionless soil with different water level elevation. J. Applied Sci., 9: 909-916.

Tresca, H., 1868. Memoire sur l'ecoulement des corps solides. Mem. Pres. Par Div. Savants, 18: 733-799.